**JST: Smart Systems and Devices**
*Volume 35, Issue 2, May 2025, 043-053*

# Analysis of the Zero-Missing Phenomenon on Mixed Overhead-Underground Cables in 220 kV Transmission Lines

***Pham Thanh Chung**, Tran Van Top***
*Hanoi University of Science and Technology, Ha Noi, Vietnam*
**Corresponding author email: chung.phamthanh1@hust.edu.vn*

**Abstract**

*The paper investigates the dynamic behavior of a 220 kV mixed overhead-underground transmission line compensated with a shunt reactor, with a focus on the current zero-missing phenomenon and switching overvoltages. The zero-missing phenomenon, a condition in which the current through the circuit breaker fails to reach zero, can affect breaker operation and system stability, particularly in shunt-compensated systems. Key factors influencing this issue include cable length, cable configuration, reactive power compensation, and switching strategies. Using EMTP/ATP simulations based on a real grid model, the study evaluates various mitigation strategies for the zero-missing phenomenon, such as pre-insertion resistors, compensation ratios, and connections to high-power loads. Transient overvoltages on cable cores and sheaths during switching operations are also analyzed.*

Keywords: The zero-missing phenomenon, shunt reactor, mixed transmission lines, switching overvoltage.

## 1. Introduction

Long High Voltage Alternating Current (HVAC) cables are now being researched by several system operators, or they have already planned to employ them in future transmission grid expansions. When long cables are being used, shunt reactors (SRs) are required for reactive power adjustment in order to keep the voltage within permissible limits. Shunt reactors should normally be connected directly to the wire and turned on with the cable in order to lower switching overvoltages and control the capacitive current in the line breaker, particularly for long cable lengths [1, 2].

The zero-missing phenomenon occurs when the alternating current fails to cross zero for several cycles, preventing the circuit breaker (CB) from opening safely without specialized interruption devices [3, 4]. High-voltage underground cables (HV UGCs), due to their large capacitive effects, require shunt reactors for reactive power compensation. This phenomenon has been observed at 150 kV [4], 380 kV in the Netherlands [1], and 550 kV in Japan [3]. Under no-load conditions, the SR current is nearly out of phase with the cable charging current, reducing the AC component through the CB [5, 6]. However, the SR current also includes a transient DC component, which may dominate the total current and delay zero crossing until it decays [3, 7]. When the CB closes on an unloaded cable with low SR resistance, a large time constant can cause the zero-missing phenomenon to persist for several seconds, depending on the closing instant [8].

Countermeasures for the zero-missing phenomenon in HVAC cable systems are generally categorized as prevention, mitigation, or handling methods [1, 8]. Preventive strategies aim to avoid the phenomenon entirely, such as connecting the shunt reactor at the voltage peak or using pre-insertion resistors to damp the DC component [7, 8]. Sequential energization, by delaying the energization of the cable and shunt reactor is also effective. Mitigation measures reduce the severity or duration, often by enhancing DC offset damping, typically with pre-insertion resistors. Handling approaches manage the system once zero-missing occurs, such as sequential switching after faults [1].

Studies highlight the effectiveness of voltage-peak switching and pre-insertion resistors in eliminating the phenomenon [8, 9]. Electromagnetic transient simulations, primarily using PSCAD/EMTDC for its accurate frequency-dependent modeling of high-voltage underground cables, are widely applied [1, 8-9]. EMTP-RV is also used to analyze the conditions leading to zero-missing events [4].

This paper investigates the zero-missing phenomenon in 220 kV transmission lines in Vietnam and proposes mitigation strategies. The main contributions are:

- Simulation of the zero-missing phenomenon at the 220 kV level using EMTP/ATP and comparison with other software tools;

ISSN 2734-9373
https://doi.org/10.51316/jst.182.ssad.2025.35.2.6
Received: Dec 17, 2024; revised: Mar 19, 2025
accepted: Apr 15, 2025

- Analysis of different transmission line configurations, including fully underground and mixed overhead–underground systems;
- Evaluation of cable layout effects (horizontal, vertical, and triangular arrangements);
- Assessment of key influencing factors such as shunt reactor (SR) compensation ratio, underground cable length, CB switching time, and SR placement at both ends;
- Proposal of mitigation measures using pre-insertion resistors with varying values and connection to large fluctuating loads;

The paper is organized as follows: Section 1 introduces the topic; Section 2 describes the zero-missing phenomenon and influencing parameters; Section 3 presents mitigation strategies; and the final section discusses the impact of placing SRs at both ends of the line.

## 2. The Zero-Missing Phenomenon

The zero-missing phenomenon can be illustrated using a parallel LC circuit with equal impedance, where the capacitor and inductor currents are equal in magnitude but opposite in phase. A DC component may appear in the inductor current depending on the switching instant [8].

Since the inductor current lags the voltage by 90°, it peaks when the voltage is zero. To maintain current continuity at the switching moment, a DC component is introduced if the inductor is connected at zero voltage-equal in magnitude to the AC component. In contrast, no DC offset occurs if the connection is made at the voltage peak [10].

In ideal conditions without resistance, the DC component persists indefinitely. However, in real systems, resistance causes it to decay gradually over time

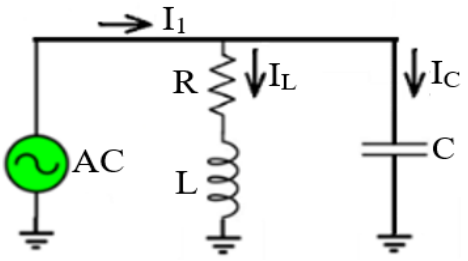


Fig. 1. RLC parallel circuit: inductor and resistor in series, in parallel with a capacitor

Fig. 1 shows a circuit with an inductor in series with a resistor, connected in parallel with a capacitor. The resistor's value is 100 times smaller than the inductor's reactance, which is equal to that of the capacitor. Fig. 2 illustrates the currents through the inductor ($I_L$), the capacitor ($I_C$), and their sum ($I_1 = I_L + I_C$). When the circuit breaker (CB) closes at zero voltage, a maximum DC component is generated. The AC components of $I_L$ and $I_C$ cancel each other, leaving only a decaying DC current.

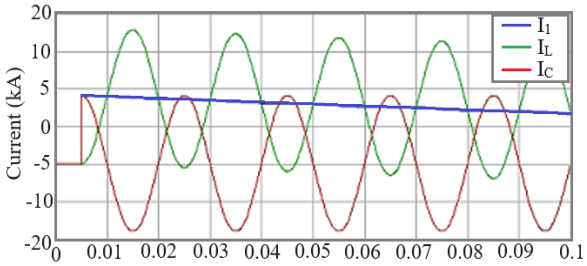


Fig. 2. Currents through the inductor ($I_L$), capacitor ($I_C$), and their sum ($I_1 = I_L + I_C$)

A system comprising a shunt reactor (SR) and a cable behaves similarly to this configuration. The cable acts mainly as a capacitive shunt due to its dominant capacitance, while the SR can be modeled as an inductor in series with a resistor [11].

However, unlike the simplified RLC circuit, the real cable–SR system also experiences switching overvoltages caused by energy oscillations between the cable's capacitance and inductance during energization [12]. To limit these overvoltages, switching should occur near the voltage peak. Conversely, minimizing the zero-missing phenomenon requires careful control of the switching instant, as the connection voltage significantly affects its severity [13].

### *2.1. Simulation Model*

The transmission project connects two sources via a 220 kV HVAC single circuit, with rated capacities of 231 MVA at Hoa Binh Substation and 165 MVA at Tay Hanoi. The simulation model represents a 220 kV mixed transmission line, consisting of a 30 km Cross-Linked Polyethylene (XLPE) cable segment between two overhead line sections totaling 20 km, as shown in Fig. 3. Both 220 kV sources are modeled using Thevenin equivalent circuits, with parameters listed in Table 1. Cable and overhead line data are based on standard specifications for 220 kV lines in the Vietnam power grid, as described in [14].

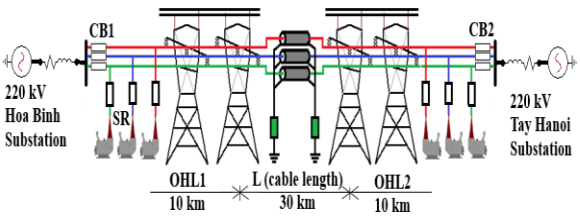


Fig. 3. System model

Table 1. Equivalent source characteristics

| Location | R (Ω) | X (Ω) |
|---|---|---|
| Hoa Binh | 0.33 | 2.17 |
| Tay Hanoi | 0.6 | 2.9 |

Table 2. Parameters of Cu-XLPE-1200 mm$^2$ cable

| | | | |
|---|---|---|---|
| $r_2$ | 12.54 mm | $\varepsilon_{r1}$ | 3.5 |
| $r_3$ | 22.735 mm | $\varepsilon_{r2}$ | 2.0 |
| $r_4$ | 26.225 mm | $\rho_c$ | $1{,}7.10^{-8}$ Ωm |
| $r_5$ | 29.335 mm | $\rho_s$ | $2{,}1.10^{-7}$ Ωm |

The single cable line (CL) configuration consists of three 1200 mm² copper cores with 220 kV XLPE insulation. These cables are arranged horizontally, spaced 0.5 m apart, and buried 1.5 m below ground. Table 2 summarizes the geometric, physical, and structural properties of the underground cable line, along with the data used in the EMTP-ATP simulation, shown in Fig. 4.

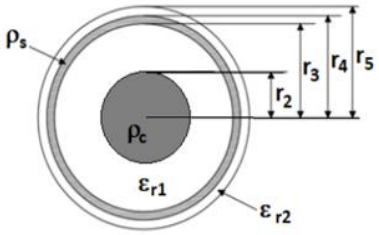


Fig. 4. Schematic of the underground cable structure

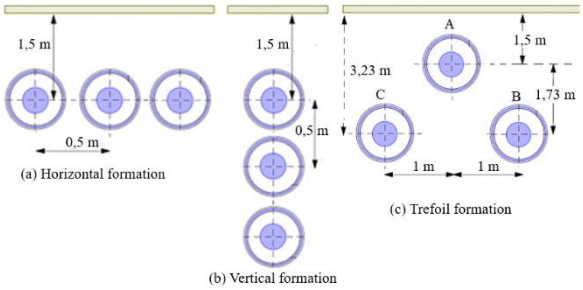


Fig. 5. Structure of the underground cable

Cables are typically arranged either horizontally (Fig. 5a) or vertically (Fig. 5b) when buried directly in the ground for construction convenience. However, this layout causes unbalanced mutual impedance between phases, with the center cable accumulating more heat, which reduces its current-carrying capacity. Alternatively, cables installed in tunnels are often arranged in a triangular (trefoil) formation (Fig. 5c) to address the limitations of horizontal configurations. Since cable arrangement affects capacitance, inductance, wave reflections, and induced currents on the sheath, these factors are considered in the zero-missing phenomenon calculations.

The study used the Bergeron model, despite its limitations in simulating long underground cables, as it calculates wave impedance and wave propagation at a fixed frequency, where parameters such as attenuation coefficient, wave propagation velocity, and wave impedance of the core and sheath converge between phases [15]. The Bergeron model is a simple, constant-frequency method based on travelling wave theory, treating the line as lossless with distributed series resistance lumped at both ends of the line [16]. This model is suitable for underground cable configurations with a conductive core and an outer sheath, allowing accurate calculation of wave propagation while accounting for attenuation with added resistive components. Despite its limitations, it is preferred for very long transmission lines due to its simplicity and low computational demand.

Both ends of the cable sheath are directly grounded, as shown in Fig. 6. The grounding resistance at each tower ($R_e$) is considered to be 10 Ω, and the grounding resistance at the junction point between the tower and the cable sheath is connected to the cable's grounding system [17].

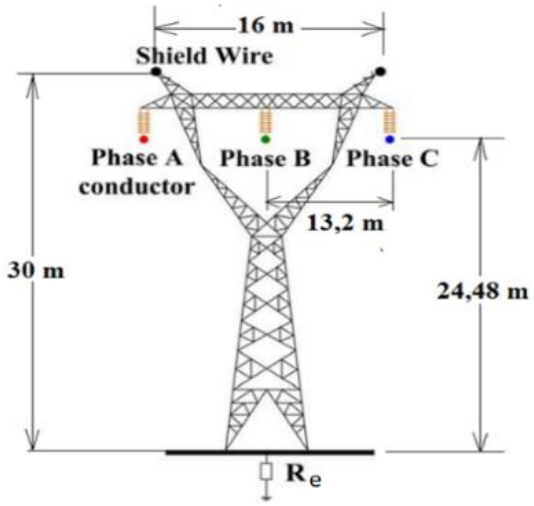


Fig. 6. Outline of simulated 220 kV OHL tower

All overhead line (OHL) towers are grounded using a 50 Hz grounding system, as shown in Fig. 6. Lightning protection wire used is a Tk 70 with an outer radius $r_{out}$ of 5.5 mm and a DC resistance $R_{DC}$ of 0.77 Ω/km. The ACSR 400/64 conductor has an outer radius $r_{out}$ of 13.85 mm, an inner radius $r_{in}$ of 7.6 mm, and a DC resistance $R_{DC}$ of 0.0741 Ω/km.

Shunt reactors are modeled as inductors in series with resistors, while the cable is primarily modeled as a capacitive element [2, 11].

The SR parameters are defined according to . followy expressions:

$$L_S(H) = \frac{1}{4\pi^2 f^2 C}$$

$$R_S(W) = 0{,}2328 L_S$$

Compensation level: $K = \frac{Q_{L_{Shunt}}}{Q_{C_{cable}}} = \frac{1}{\omega^2 L_S C}$ (1)

$$\rightarrow L_s(H) = \frac{1}{\omega^2 K C}$$

$$Q_{L\_Shunt}(MVAR) = \frac{U_m^2}{X_L} = \frac{U_m^2}{\omega L_s}$$

$$Q_{C\_Cable}(MVAR) = \frac{U_m^2}{X_C} = U_m^2 \omega C$$

where: $L_S$ is the inductance of the SR (H), $R_S$ is the resistance of the SR (Ω), $C$ is the capacitance of the cable (F), $f$ is the industrial frequency (Hz), and $U_m$ is the rated voltage of the transmission lines (kV).

### 2.2. Full Underground Cable Scenario

*2.2.1. Simultaneous closing of all three phases*

For a 50 km underground cable with 100% compensation, the parameters from (1) are: $C=1.05.10^{-5}$ *F*, $L_S=0.97$ *H*, $R_S=0.22$ *Ω*. Assuming a circuit breaker (CB1) closing time of 5 ms, the total current through CB1 (Fig. 9) is the sum of the cable core current (Fig. 7) and the shunt reactor current (Fig. 8).

The zero-missing phenomenon occurs approximately 5 ms after closing for phase A, 15.8 ms for phase B, and 14.6 ms for phase C. A high *X/R* ratio exacerbates the phenomenon, as the DC component decays more slowly, prolonging the absence of current zero crossings. The peak current through CB1 reaches $I_{peak}$ = 4.2 kA.

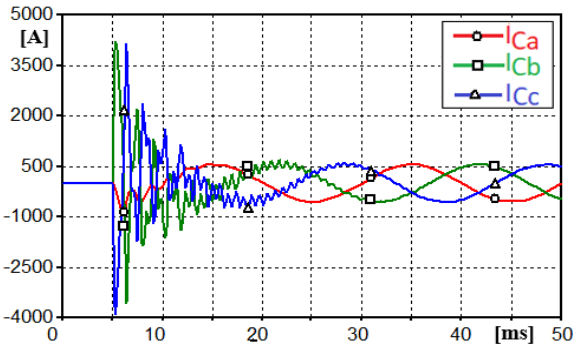


Fig. 7. Current through the cable cores

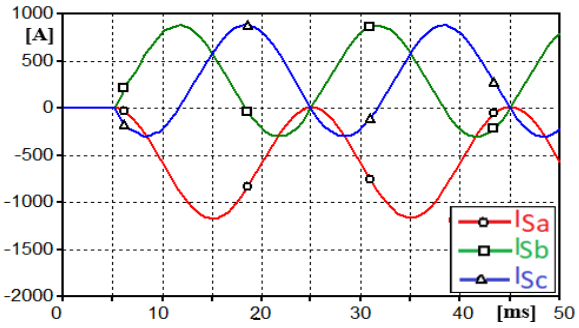


Fig. 8. Current through the SR

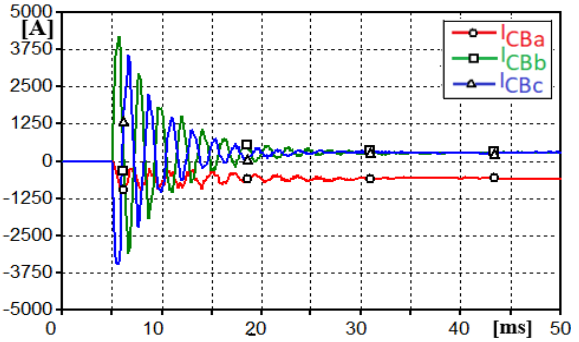


Fig. 9. Total current through CB1 ($I_{CB}=I_C+I_S$)

Switching overvoltages, as illustrated in Fig. 10, arise from energy oscillations between the cable's capacitance and inductance. Their magnitude depends on the voltage at the instant the cable and shunt reactor are energized. In phase B, the peak overvoltage reaches $V_{peak}$=354 kV (1.97 p.u), highlighting the importance of accurate switching timing to mitigate overvoltage risks.

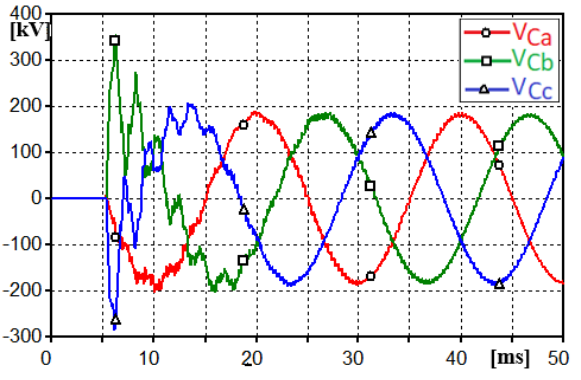


Fig. 10. Switching overvoltage on the cable cores at the cable termination

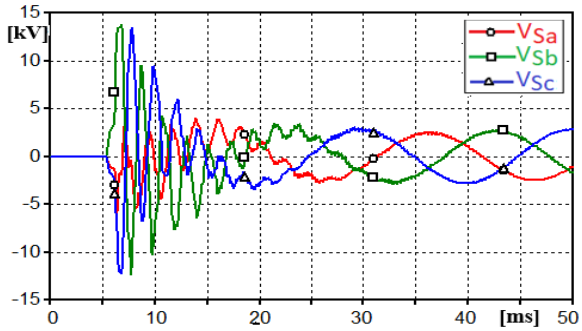


Fig. 11. Induced voltage on the cable sheath at the cable termination point

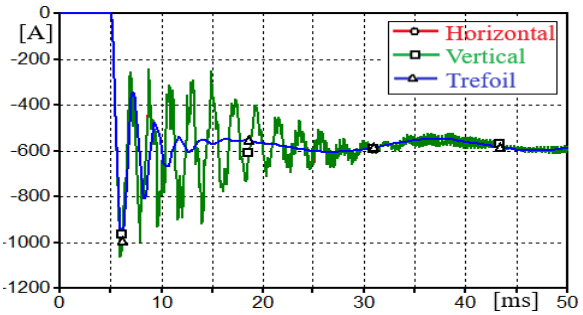


a. Current through CB1 of phase A

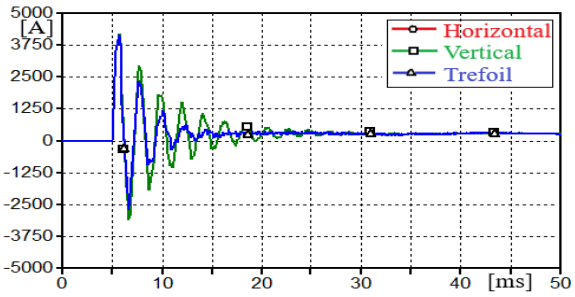


b. Current through CB1 of phase B

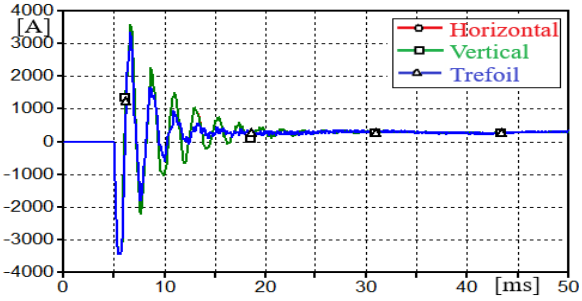


c. Current through CB1 of phase C

Fig. 12. Current through CB1 for different cable configuration

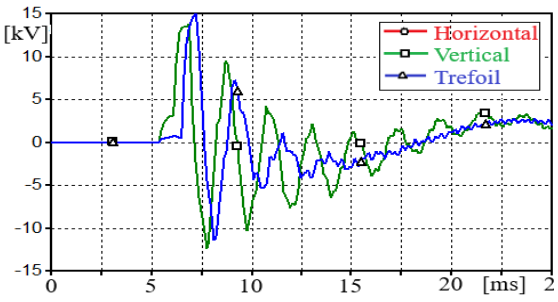


Fig. 13. Induced voltage on the cable sheath (Phase B) at the cable termination for different configurations

Due to the cable's considerable length and the connection between the cable sheath grounding resistance and the tower grounding system, the maximum induced voltage on the cable sheath at the end of the cable (Fig. 11) reaches 13.7 kV. This remains below the basic lightning impulse insulation level (BIL) of 40 kV for 220 kV cable sheaths [17], emphasizing the need for appropriate design and protection measures to ensure sheath integrity.

A comparison of underground cable configurations-horizontal, vertical, and triangular-reveals that horizontal and vertical placements have negligible impact on the zero-missing phenomenon and sheath overvoltage [14] (Fig. 12). In contrast, the triangular configuration yields the fastest current attenuation (Fig. 12bc). Although it initially exhibits higher oscillations, these decay rapidly, and the zero-missing phenomenon occurs earlier due to the configuration's lower capacitance and higher inductance. The maximum induced voltage on the cable sheath reaches 15 kV, exceeding the 13.7 kV observed in horizontal and vertical placements (Fig. 13).

*2.2.1 Staggered circuit breaker closing*

By offsetting the CB closing times across phases phase A at 5 ms, phase B at 11.6 ms, and phase C at 8.3 ms the voltage phases are staggered by approximately 3.3 ms. As shown in Fig. 14, this method eliminates the zero-crossing points in the CB current immediately after closure. However, it significantly reduces the peak current to 1 kA, compared to 4.2 kA in the simultaneous closing scenario.

Moreover, this approach reduces the induced voltage on the cable sheath to 3.2 kV, a considerable decrease from the simultaneous closing case. The voltage on the cable core also remains nearly constant, as illustrated in Fig. 15.

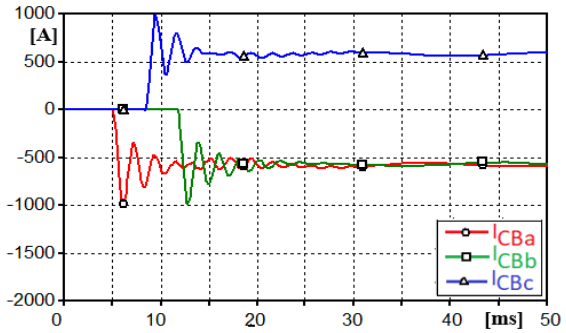


Fig. 14. Current through CB with staggered closing times for each phase

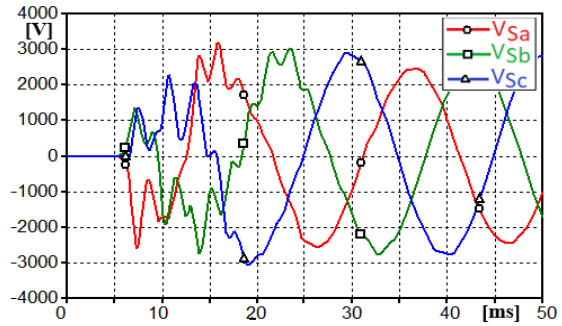


Fig. 15. Voltage on the cable core during staggered CB closing

### *2.3. Mixed Transmission Line Case*

This section examines a mixed transmission line configuration comprising both overhead lines (OHL) and underground cables (UGC). Four scenarios are considered: comparison with a fully underground line, variation in underground cable length, changes in SR compensation ratio, and the ratio of cable length to total line length.

#### *2.3.1. Shunt Reactor compensating 100% of the cable's reactive power*

Consider a mixed line consisting of a 30 km underground cable section between two 20 km overhead lines, as shown in Fig. 3. The compensation level is set to 100% of the cable's reactive power. In this setup, phase B loses its current zero-crossing after approximately 17 ms (Fig. 16), compared to 15.8 ms in the full cable configuration (Fig. 9). The peak current through the CB is reduced to 2.58 kA, lower than the 4.18 kA in the full cable case. However, the overvoltage on the cable core is also lower 342 kV (1.67 p.u) in the mixed case (Fig. 17) versus 354 kV (1.97 p.u) in the full cable case (Fig. 10). Similarly, the induced voltage on the cable sheath decreases to 10.8 kV, compared to 13.7 kV (Fig. 18). These reductions are due to the higher wave impedance of overhead lines, which leads to greater energy reflection and lower peak overvoltages during switching events [18].

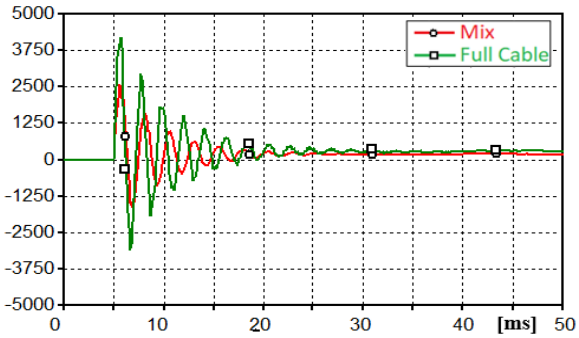


Fig. 16. Current in phase B when CB closes simultaneously

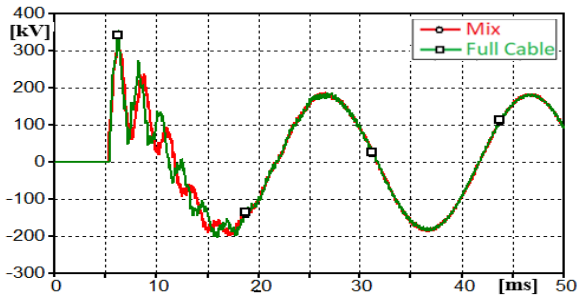


Fig. 17. Overvoltage on phase B of the cable core at the cable end

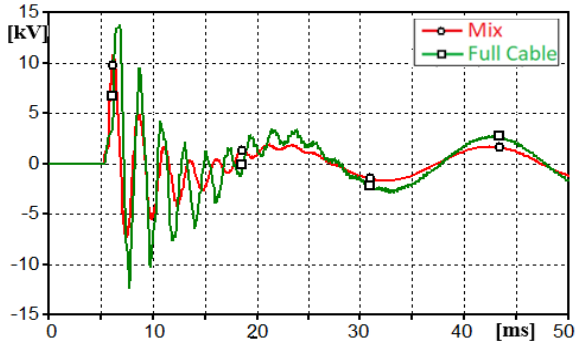


Fig. 18. Induced voltage on the cable sheath at the cable end

#### *2.3.2. Effect of cable length variation*

Following CB closure in a mixed transmission line, the zero-missing phenomenon typically appears about one cycle (~15 ms) after switching. To evaluate the influence of underground cable length, the overhead line length is fixed, while the underground cable section is varied from 5 km to 30 km.

In all scenarios, the shunt reactor (SR) compensation level is kept at 100%, and the CB closes all three phases simultaneously. The results in Fig. 19 show the relationship between cable length and the time of zero-missing occurrence.

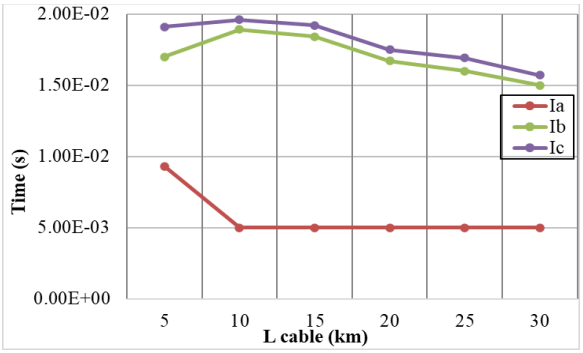


Fig. 19. Time of zero-missing phenomenon as a function of cable length

As shown in Fig. 19, phase A (Ia) demonstrates a sharp decline in zero-missing time from approximately 9 ms at 5 km, stabilizing around 5 ms from 10 km onward. In contrast, phases B ($I_b$) and C ($I_c$) initially show increased zero-missing durations, peaking between 10-15 km, before gradually decreasing as cable length increases. This trend indicates that at shorter lengths, stronger inductive effects dominate, especially in phases B and C, extending the zero-missing duration. As the cable length increases, the growing influence of capacitance alters transient behavior, helping to restore zero-crossings more quickly.

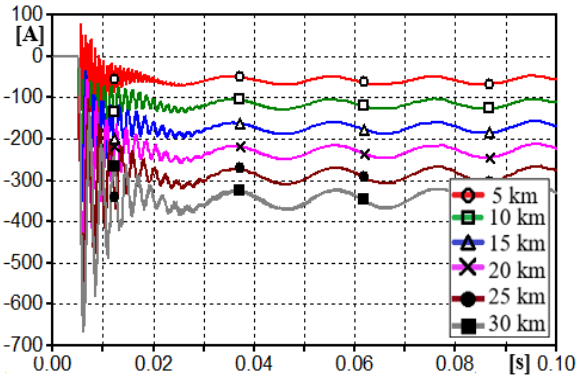


Fig. 20. Current through phase A for variable cable lengths

This behavior has important implications for circuit breaker (CB) performance, as prolonged zero-missing can delay successful fault interruption. Fig. 20 further shows that as cable length increases, both peak and steady-state current magnitudes rise. For a 30 km cable, the maximum negative current reaches around –600 A. Longer cables also exhibit more intense and sustained oscillations, pointing to stronger resonance effects from increased system capacitance and inductance.

*2.3.3. Effect of compensation factor change*

The impact of varying the shunt reactor compensation ratio was assessed at levels of 25%, 50%, 75%, and 100%. As shown in Fig. 21, the current through the circuit breaker (CB) fails to cross the zero point when compensation exceeds 50%. This is due to the increasing DC component in the current as the compensation level rises. Consequently, if compensation exceeds 50%, the CB cannot safely operate during faults, preventing proper interruption. These findings stress the importance of limiting the compensation ratio to 50% or less to ensure safe and reliable CB operation.

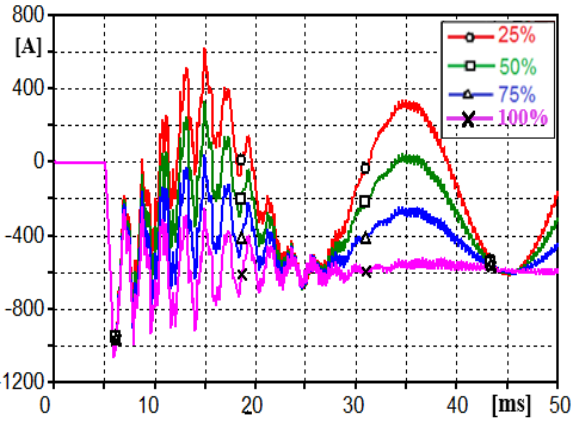


Fig. 21. Current through the CB in phase A with changing compensation levels

*2.3.4. Effect of cable length ratio*

The effect of the cable length ratio relative to the total transmission line length (50 km) was evaluated, as detailed in Table 3. This analysis assumes the CB closes when phase voltages pass through the zero point. As shown in Fig. 22, the current through the CB in phase A changes with varying cable length ratios. Results indicate that as the cable length ratio increases, the zero-missing phenomenon becomes more pronounced. This is due to the increasing capacitive effects of the cable, which amplify the DC component and delay zero-crossings. The findings underscore the importance of optimizing the cable-to-overhead line ratio to mitigate the zero-missing phenomenon and ensure reliable CB operation.

Table 3. Cable length and overhead line ratio

| Case | OHL length (km) | Cable length (km) |
|---|---|---|
| Fully OHL | 50 | 0 |
| 20% Cable | 40 | 10 |
| 40% Cable | 30 | 20 |
| 60% Cable | 20 | 30 |
| 80% Cable | 10 | 40 |
| 100% Cable | 0 | 50 |

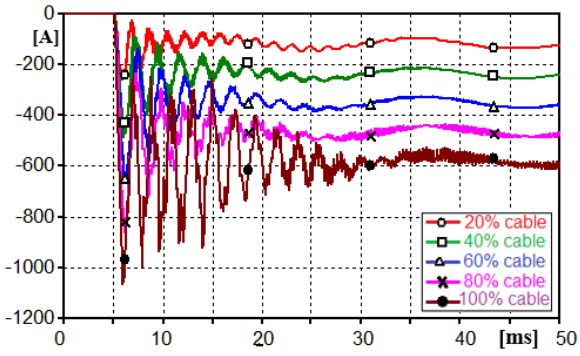


Fig. 22. Current through the CB in phase A with varying cable length ratios

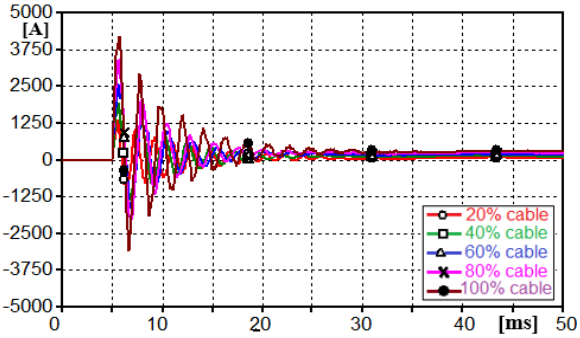


Fig. 23. Current through the CB in phase B with varying cable length ratios

Fig. 23 shows that as the underground cable length (or the cable ratio) increases, both the initial fault current and the duration of oscillations also increase. This is due to the higher system capacitance, which affects the momentary short-circuit current. Systems with a high cable ratio require more careful protection design, particularly for the fast and accurate tripping of CB.

*2.3.5. Effect of frequency variation*

Simulations were conducted at three different frequencies within the resonant range to evaluate their impact on the zero-missing phenomenon. Fig. 24 shows that while the current through the circuit breaker in phase C varies with frequency, the zero-missing phenomenon is not significantly affected. At 50 Hz, the waveform exhibits higher peak currents and longer oscillation duration. However, increasing the frequency to 500 Hz and 1 kHz leads to faster damping and reduced oscillation amplitude. Despite these differences, all cases demonstrate similar zero-crossing behavior. This indicates that although resonance frequency influences waveform shape, it does not critically alter zero-crossing dynamics. Thus, considering a range of frequencies provides more reliable insights into system behavior than focusing on the resonance point alone.

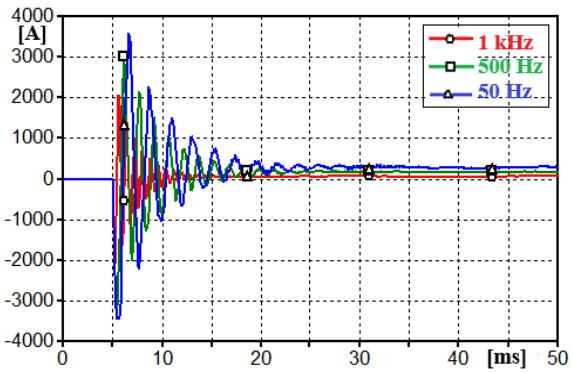


Fig. 24. Current through CB with varying frequency

## 3. Minimizing the Zero-Missing Phenomenon

The zero-missing phenomenon occurs when the significant DC component in the current does not decay quickly enough after energizing the cable lines. This issue is compensated by the SR [4, 6-8]. The low impedance, particularly when the cables are unloaded, results in a large time constant ($\tau = L/R$), which delays the decay of the DC component [8, 9]. The proposed solution is to increase the total resistance in the circuit, which reduces the time constant and allows the DC component to decay faster, enabling the current to cross the zero point sooner [1, 9].

The effectiveness of zero-missing mitigation measures, such as using pre-insertion resistors, is evaluated based on how quickly the DC component is extinguished [8]. The resistor value is typically determined by calculating the energy needed to dissipate before the circuit breaker trips, assuming 100% reactive power compensation [8]. Simulations with different pre-insertion resistor values and load capacities are used to observe the zero-missing phenomenon's duration and DC component magnitude. The goal is to reduce the DC component enough for the current to cross zero quickly, ideally before the CB's main contacts are fully closed.

### *3.1. Effectiveness of Using Pre-insertion Resistors*

According to [8], the pre-insertion resistor $R_p$ can be estimated using formula:

$$R_p(W) = \frac{2L_s}{0.01} \tag{2}$$

or calculated according to [9],

$$R_p(W) = \frac{3L_s}{0.02} \tag{3}$$

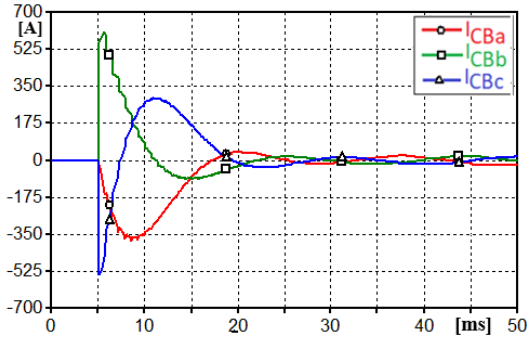


Fig. 25. Current through the CB with $R_p$=241 Ω

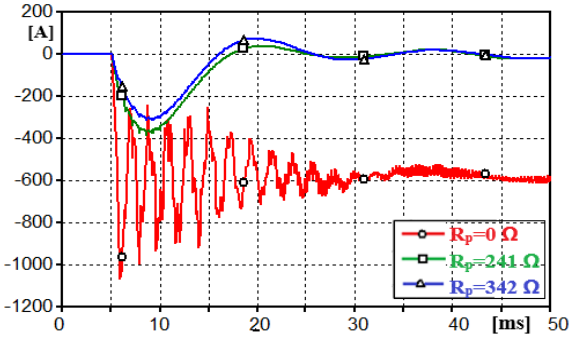


Fig. 26. Current through the CB at the phase A with variable $R_p$

The comparison of $R_p$ = 342 Ω from (2) and $R_p$=241 Ω from (3) in mitigating the zero-missing phenomenon. As illustrated in Fig. 25, when $R_p$=241 Ω, the current through CB at phase A crosses zero earlier. After closing, transient currents with peak values around 400–650 A are observed. The zero-missing phenomenon occurs at 9 ms (phase C), 11 ms (phase B), and 13 ms (phase A), indicating effective reduction. The oscillations decay rapidly and stabilize within 15 ms. Overall, using $R_p$=241 Ω significantly mitigates transients and improves current interruption performance.

The comparison of different $R_p$ values shows that higher resistance improves the suppression of the zero-missing phenomenon (Fig. 26). Without a resistor, the current in phase A exhibits strong, prolonged oscillations and fails to cross zero for an extended period. With $R_p$=241 Ω, the zero-missing phenomenon occurs earlier (~32 ms), and the oscillations are notably reduced. When $R_p$=342 Ω, the current crosses zero even earlier (~23 ms) with the lowest peak current, indicating better damping. Increasing the pre-insertion resistor value enhances current damping, speeds up the zero-missing event, and effectively mitigates the phenomenon.

Fig. 27 shows the induced overvoltage on the cable sheath at the cable end with varying $R_p$. With $R_p$=241 Ω, the voltage on the cable sheath at phase A is reduced to 2.6 kV compared to 13.7 kV when no resistor is used.

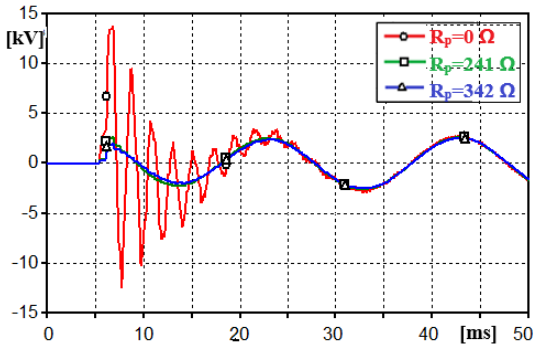


Fig. 27. Induced voltage on the cable sheath at the cable end with variable $R_p$

### *3.2. Connection to Large-Capacity Loads*

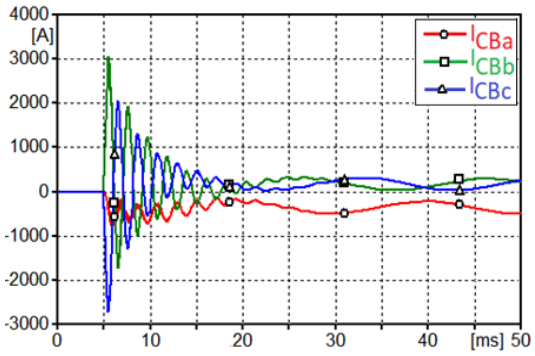


a. With a load of 100 MVA

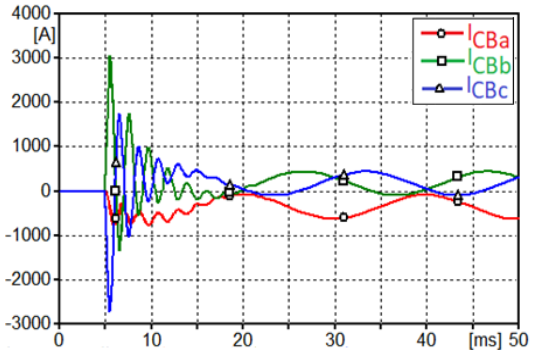


b. With a load of 200 MVA

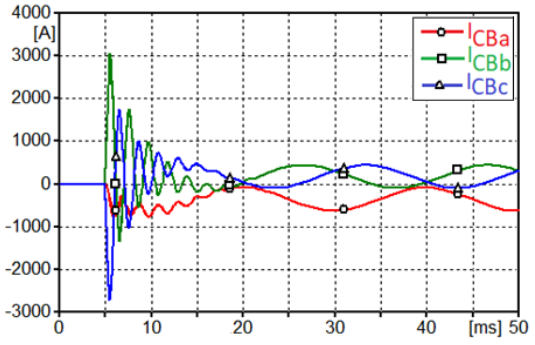


c. With a load of 300 MVA

Fig. 28. Current through CB when the transmission line connects to the load

Transmission lines connected to large-capacity loads can effectively mitigate the zero-missing phenomenon due to the significant reactive power demand. A 220 kV transmission line with a capacity ranging from 200 MVA to 300 MVA demonstrates this capability, particularly at load levels of 100 MVA, 200 MVA, and 300 MVA. The presence of a substantial load stabilizes the system, reducing the likelihood of the zero-missing phenomenon.

The analysis of current through the CB when connecting a transmission line to varying load capacities demonstrates the impact of load on mitigating the zero-missing phenomenon. For a load of 100 MVA (Fig. 28a), the zero-missing phenomenon occurs on all three phases, indicating insufficient reactive power stabilization. At a load of 200 MVA (Fig. 28b), the phenomenon is limited to phase A, showing partial improvement. Finally, with a load of 300 MVA (Fig. 28c), the zero-missing phenomenon is fully resolved across all phases, confirming that higher-capacity loads effectively eliminate the issue and enhance system stability.

## 4. Compensation at Both Ends

The simulation model incorporates two power sources connected at either end of the mixed transmission line (Fig. 3). The compensation level at each end is often balanced to maintain system stability, with the total compensastion across both ends being 50%. The resistance engagement times are set to 5 ms and 10 ms, with SR parameters defined as: $C$=6,3.10$^{-6}$ F, $L_S$=6,44 H, $R_S$=1,5 Ω.

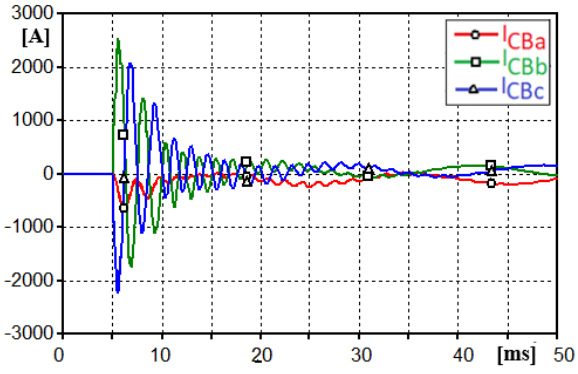


Fig. 29. Current through CB1 with a total compensation capacity of both ends equal to 50%

The results show that with the total compensation capacity for both sides below 50%, the zero-missing phenomenon will not occur on all 3 phases of CB1 (Fig. 29) and will occurs in the case of the total compensation capacity reaching 100% (Fig. 30).

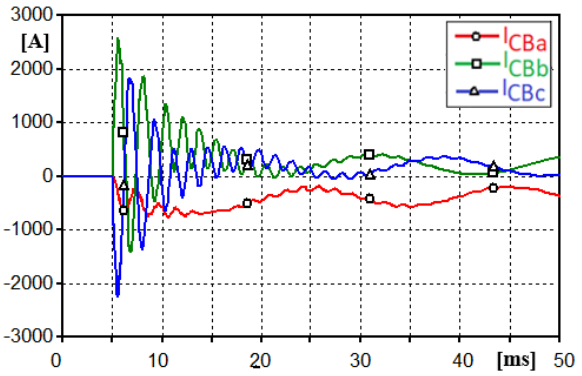


Fig. 30. Current through CB1 with a total compensation capacity of both ends equal to 100%

## 5. Conclusion

The analysis highlights the challenges posed by the zero-missing phenomenon in mixed overhead-underground transmission lines, particularly its impact on circuit breaker (CB) operation and system reliability. Key findings from this study demonstrate that cable length, compensation levels, and switching strategies significantly influence the severity of the phenomenon. Several mitigation strategies—such as using pre-insertion resistors, optimizing compensation ratios, and connecting large-capacity loads—can effectively reduce the impact of the zero-missing phenomenon.

The study also reveals that while overvoltages on the core and sheath of the cable occur, they do not endanger the insulation of the cable when the zero-missing phenomenon is present. Moreover, the results suggest that while resonant frequencies can affect the waveform shape, they do not significantly alter the zero-crossing behavior. Compensation at both ends of the transmission line offers a balanced approach to minimizing the zero-missing phenomenon and ensuring the safe operation of the system.

These findings emphasize the importance of careful system design and operational planning to address the complexities of modern transmission systems. However, it is important to note that the study results have not been evaluated for asymmetric transmission line configurations, meaning that individual values of $L_s$ and $R_p$ should be considered in such cases. Additionally, the study focuses on a specific line in Vietnam operating at a single voltage level of 220 kV, without delving into power systems with different voltage levels, characteristics, or operating conditions. Future studies will explore the impact of system structure and variables—such as voltage, power frequency, short-circuit power, and $X/R$ factor—on the zero-missing phenomenon.

**Acknowledgments**

This research is funded by Hanoi University of Science and Technology (HUST) under project number T2024-PC-066.

**References**

[1] H. Khalilnezhad, M. Popov, L. van der Sluis, J. A. Bos, J. P. W. de Jong and A. Ametani, Countermeasures of zero-missing phenomenon in (E)HV cable systems, IEEE Transactions on Power Delivery, vol. 33, iss. 4, pp. 1657-1667, Jul. 2017. https://doi.org/10.1109/TPWRD.2017.2729883

[2] C. L. Bak, W. Wiechowski, K. Søgaard, and S. D. Mikkelsen, Analysis and simulation of switching surge generation when disconnecting a combined 400kV cable/overhead line with shunt reactor in International Conference on Power System Transients (IPST) 2007, Jun. 2007.

[3] Kobayashi, T., Eto, A., Koshizuka, T., Nishiwaki, S., Kudo, K., Matsushita, K., & Hosokawa, O., Current zero missing phenomena caused by DC current which flows from shunt reactor at the ground fault and its interruption, IEEJ Transactions on Power and Energy, vol. 127, no.1, pp. 277-283, 2007. [In Japanese: 小林 隆幸, 衛藤 淳, 腰塚 正, 西脇 進, 工藤 喜悦, 松下 耕三, 細川 修 系統事故時の直流性リアクトル放電電流の遮断器電流遮断現象, 2007 年 127 巻 1 号 pp. 277-283]. https://doi.org/10.1541/ieejpes.127.277

[4] D. Spathis, T. Boutsika, J. Prousalidis, K. Tsirekis, J. Kabouris and A. Georgopoulos, Zero missing effect transient analysis on the 150 kV AC interconnection between Crete and Peloponnese, in 2018 IEEE International Conference on High Voltage Engineering and Application (ICHVE), Athens, Greece, pp. 1-4, Sep. 2018. https://doi.org/10.1109/ICHVE.2018.8642102

[5] Munji K., Horne J., Hesselbaek B., Negra N. B., Sahukari S., & Cotter G,, Assessment and mitigation of zero missing phenomenon for compensated cables and harmonic filters, in 5th IET International Conference on Renewable Power Generation (RPG 2016), UK, 2016. https://doi.org/10.1049/cp.2016.0567

[6] Da Silva, F. Faria, and Claus L. Bak, Zero-missing phenomenon after fault clearing, in International Conference on Power Systems Transients, 2019.

[7] F. Faria da Silva, C. L. Bak, U. S. Gudmundsdóttir, W. Wiechowski, and M. R. Knardrupgård, Use of a pre-insertion resistor to minimize zero-missing phenomenon and switching overvoltages, in 2009 IEEE Power & Energy Society General Meeting, Calgary, AB, Canada, pp.1-7, Jul. 2009 https://doi.org/10.1109/PES.2009.5275992

[8] F. F. da Silva, C. L. Bak, U. S. Gudmundsdottir, W. Wiechowski, and M. R. Knardrupgaard, Methods to minimize zero-missing phenomenon, IEEE Transactions on Power Delivery, vol. 25, iss. 4, pp. 2923-2930, Oct. 2010. https://doi.org/10.1109/TPWRD.2010.2045010

[9] Linnet A, Eliminating zero-missing phenomenon in long, high voltage, underground cables, Stockholm, Sweden, 2019.

[10] J. F. Borges Da Silva, Electrotecnia Theoretical Parte, 2nd ed.. Portugal: AEIST, 1995.

[11] J. H. R. Enslin, Y. Hu, and R. A. Wakefield, System considerations and impacts of AC cable networks on weak high voltage transmission networks, in 2005/2006 IEEE/PES Transmission and Distribution Conference and Exhibition, Dallas, TX, USA, May 2006, pp. 1030–1034. https://doi.org/10.1109/TDC.2006.1668644

[12] A Greenwood, Electric Transients in Power Systems, 1st ed. New York, USA: Wiley, 1971.

[13] Y. H. Fu and G. C. Damstra, Switching transients during energizing capacitive load by a vacuum circuit breaker, IEEE Transactions on Electrical Insulation, vol. 28, iss. 4, pp. 657-666, Aug. 1993. https://doi.org/10.1109/14.231549

[14] P. T. Chung, P. H. Thinh and T. V. Top, Effect of cable configuration on overvoltage on cable sheath in “mix” transmission lines, JST: Engineering and Technology for Sustainable Development, vol. 1, iss. 2, Apr. 2021, 001-006. https://doi.org/10.51316/jst.149.etsd.2021.31.2.1

[15] P. T. Chung, Research on overvoltage on mixed overhead line and cable transmission system, PhD thesis, Hanoi University of Science and Technology, 2023. [In Vietnamese: Nghiên cứu quá điện áp trên hệ thống truyền tải hỗn hợp đường dây trên không và cáp, Luận án tiến sĩ, Đại học Bách Khoa Hà Nội, 2023].

[16] H. W. Dommel, EMTP Theory Book, Microtran Power System Analysis Corporation. Vancouver: British Columbia, 1996.

[17] IEEE Guide for Bonding Shields and Sheaths of Single-Conductor Power Cables Rated 5 kV Through 500 kV, IEEE Standard, vol. 575, Sep. 2014.

[18] A. Ametani, Wave propagation characteristics of cables, IEEE Transactions on Power Apparatus and Systems, vol. PASS-99, iss. 2, pp. 499-505, Mar. 1980. https://doi.org/10.1109/TPAS.1980.319685